CHINESE JOURNAL OF PHYSICS VOL. 52, NO. 5 October 2014

High Pressure Elastic Properties of Wurtzite Aluminum Nitrate

E. Güler* and M. Güler

Department of Physics, Hitit University, 19030 Corum, Turkey
(Received April 2, 2014)

Aluminum nitrate is an indisputable material for current optoelectronic technology. Although much scientific effort has been devoted to understand the ground state elastic properties of aluminum nitrate, little is known about the high pressure elastic behavior of this crucial material. In contrast to previous theoretical methods, we present an application of a shell model interatomic potential for the first time in conjunction with geometry optimization calculations to predict some elastic and relevant properties of wurtzite aluminum nitrate (w-AlN) under pressures up to 50 GPa. The obtained ground state results for the elastic constants, Poisson ratio, elastic wave velocities, and dielectric optical constants agree well with the existing experimental values, and better than those of some theoretical data. In addition, the bonding character of w-AlN are found to be ionic for the entire pressure range, whereas elastic isotropy arises for the pressures below 10 GPa. In conclusion, application of shell model potentials to the high pressure properties of w-AlN offers satisfactory results, and these results can be useful for the future experimental and theoretical works on related material under pressure.

DOI: 10.6122/CJP.20140610A PACS numbers: 62.20.D-, 62.50.-p, 77.84.Bw, 81.05.Ea

I. INTRODUCTION

In the past few decades, the computational modeling of materials has been an efficient and quick tool to address the unclear issues of physical interest. The results of these computations help to predict new materials and can replace experiments that are quite expensive and even impossible in the laboratory [1, 2].

Further, predicting good elastic and thermodynamic properties of materials is an attractive subject for current solid sate science and industry. In particular, these properties at high pressure and temperature are most significant in many modern technologies [3].

The subject of the present work is the material AlN, which is a prominent member of the III-V semiconductor family (GaN, AlN, and InN). From a crystallographic outlook, under ambient conditions, AlN crystallizes in the wurtzite crystal structure (w-AlN) with $P6_3mc$ space group. Therefore, w-AlN is the most observed structure during experiments, in contrast to the difficultly fabricated of the cubic zinc blende and rock salt phases. Noteworthy to mention here, AlN has the largest direct band gap with 6.3 eV, that makes AlN an ideal candidate for developing optoelectronic technology to construct violet region devices [4–6]. In addition, AlN is one of the best thermal conductors, with a low ther-

*Electronic address: eguler71@gmail.com

mal expansion coefficient. Several other uses of AlN cover surface acoustic wave devices, integrated circuit packaging, ignition modules, radio frequency and microwave packages, heat sinks, laser diodes heat spreaders, and cutting tools [7]. Scientists recognized the technological importance of AlN in the middle of the 1980s.

There have been a number of studies related to the elastic properties of w-AlN both theoretical and experimental. Tsubouchi and coworkers [8] first reported the experimental results of the w-AlN from surface acoustic wave measurements in 1985. Later, in 1993, Mc-Neil and colleagues obtained the elastic constants of w-AlN from Brillouin scattering experiments [9]. Afterwards, computations have been performed (e.g., Wright *et al.* [10], Schilf gaarde *et al.* [11], Saib *et al.* [12], Peng *et al.* [13], and Wang *et al.* [14]) to settle generally the ground state ($P = 0$ GPa and $T = 0$ Kelvin) elastic constants of w-AlN with the density functional theory (DFT) method through various interatomic potentials. However, little is known about the high pressure elastic properties of w-AlN. As far as we know, Ref. [6] is the only DFT attempt considering the high-pressure elasticity of w-AlN at $T = 0$ under high pressures.

The present inquiry, therefore, focuses on the high-pressure elastic and some other relevant properties of w-AlN. In contrast to the above existing literature methods and applied potentials, this is the first report regarding the application of a shell model potential to determine the high-pressure elastic and other related properties of w-AlN with geometry optimization calculations. During the research, we focused on the pressure behavior of five independent elastic constants and calculated bulk, shear, and Young moduli, Poisson ratio, elastic wave velocities, elastic anisotropy parameter, Kleinman parameter, static and high frequency dielectric constants, and the mechanical stability conditions of w-AlN under pressures between 0 GPa and 50 GPa at $T = 0$ K.

The rest of the paper is organized as follows. Section II gives a brief overview for geometry optimization and computational details. Section III provides the present and former results on the considered parameters of w-AlN with a discussion, and Section IV summarizes the main findings of this research in the conclusions.

II. COMPUTATIONAL DETAILS

Geometry optimization is an efficient and convenient method in both classical physics based molecular dynamics (MD) and quantum mechanics based DFT techniques to get a stable configuration for a molecule or periodic structure through fast and inexpensive energy computations. An optimization procedure involves the repeated sampling of the potential energy surface until the potential energy reaches a minimum where all forces on all atoms are zero. Many details about the optimization methods and other points of concern are explained in [15–17].

All geometry optimization calculations have been done with the General Utility Lattice Program (GULP) MD code with version 4.0. [18, 19]. This handy code allows wide-range property calculations for 3D periodic solids, 2D surfaces, and gas phase clusters by applying a proper interatomic potential depending on the demands of the research [16].

The accuracy and the reliability of the computer simulations depend on the quality of the employed interatomic potentials [20]. Moreover, shell model interatomic potential models provide satisfactory results on the ground state as well as high-pressure properties of oxides, fluorides, and other compounds [21–24]. Since the shell model and its methodologies are well established, we give only a brief description here. In this model, most of the potentials consist of Coulomb and pairwise short-range interactions with ionic polarization treated by Dick and Overhauser [25]. In addition, an atom is represented by two separate components: the core (representing the nucleus and core electrons) and the shell (representing the valence electrons). The core and the shell separately interact with other atoms and with each other. This interaction energy is represented by the short-range Buckingham energy,

$$U_{ij}^{\text{Buckingham}} = A \exp\left(-\frac{r_{ij}}{\rho}\right) - \frac{C}{r_{ij}^6},$$

where A, ρ, and C are specific interaction parameters. For further details and other assumptions, interested readers are referred to Refs. [20–25] for more about the shell model potentials and their outcomes.

An existing shell model interatomic potential [26] was employed for the to present computations, which was originally derived for the bulk and defect properties of III-V nitrides. Since w-AlN is the most observed experimental structure, a special importance is given to the ground state properties of this structure during the present inquiry to achieve a comparison with experiments. The cell parameters of w-AlN were assigned as: $a = 3.11$ Å and $c = 4.97$ Å. To obtain a successful geometry optimization without constraints [15], constant pressure optimization was used in this study. The geometry of the cells were optimized via the Newton–Raphson method based on the Hessian matrix calculated from the second derivatives, in which the Hessian matrix was recursively updated during optimization using the the BFGS algorithm [27–30] as implemented in GULP. After setting the prerequisites for w-AlN, multiple runs have been applied at zero Kelvin (0 K) temperature by checking the pressure ranges starting from 0 GPa up to 50 GPa in steps of 5 GPa.

III. RESULTS AND DISCUSSION

The elastic constants of materials afford precious and essential knowledge about many mechanical and physical properties of materials. Once the elastic constants are obtained, one may get a deeper perception on the stability of the concerned material [1, 2, 16, 17]. These constants are also informative regarding the properties of materials, e.g., interatomic bonding, equation of state, and phonon spectra. They also link to several thermodynamic parameters, such as the specific heat, thermal expansion, Debye temperature, and Grüniesen parameter, etc. However, in general, elastic constants derived from the total energy calculations correspond to single crystal elastic properties. On the other hand, the Voigt-Reuss-Hill approximation is a reliable scheme for polycrystalline materials [1, 2, 31, 32]. To determine the correct values of elastic constants and other surveyed parameters for w-AlN,

the Voigt-Reuss-Hill values were taken into account for the present research.

In a wurtzite type material, five independent elastic constants exist as: C_{11}, C_{12}, C_{13}, C_{33}, and C_{44}.

The plot in Fig. 1 compares our results and the recent DFT data [6] for the C_{11}, C_{12}, C_{13}, C_{33}, and C_{44} elastic constants of w-AlN between 0 GPa and 50 GPa.

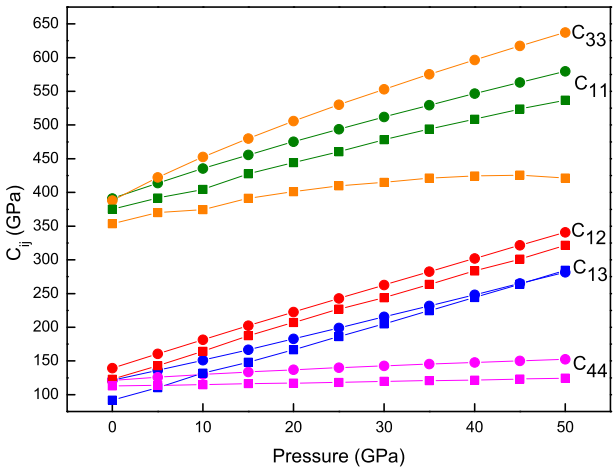

FIG. 1: A comparison for the elastic constants of w-AlN.

The closed circles denote our results, whereas squares denote the compared DFT data. At first, the obtained results show a similar trend with DFT data [6], except for a deviation for the C_{33} elastic constant. Moreover, all the obtained elastic constants of w-AlN increase with pressure except C_{44}. Beyond these increments, a closer inspection reveals that the elastic constants are in the range of $C_{33} > C_{11} > C_{12} > C_{13} > C_{44}$, and similar to the both experiments and DFT results [6, 8, 9]. Besides, Table I also lists a numerical comparison of these present results for the elastic constants with respect to some previous experimental and theoretical results. As can be seen from Table I, the present results of the ground state elastic constants are very close to the Brillouin spectroscopy measurements [9], and are better than those of former theoretical reports [6, 11–14].

From the stability outlook, the traditional Born mechanical stability condition for a hexagonal structure also holds for wurtzite crystal and must satisfy [31]

$$C_{44} > 0,\ C_{11} > C_{12} \text{ and } (C_{11} + 2C_{12})C_{33} - 2C_{13}^2 > 0.$$

Current research results for the obtained elastic constants of w-AlN satisfy the mechanical stability condition (Fig. 1 and Table I). This result points out that w-AlN is mechanically stable at 0 K and 0 GPa.

The bulk modulus (B) is the unique elastic constant of matter that divulges much information about the bonding strength. As well, it is a measure of the matter's resistance

TABLE I: Comparing the elastic constants of w-AlN with the previous and present results.

	Ref. [6]	Ref. [8]	Ref [9] Exp.	Ref. [11]	Ref. [12]	Ref. [13]	Ref. [14]	Present
C_{11} (GPa)	375.2	345	410.5 ± 10	388	376	376	376	390.9
C_{33} (GPa)	353.6	395	388.5 ± 10	458	411	354	355	387.9
C_{44} (GPa)	112.9	118	124.6 ± 4.5	99	122	115	112	121.2
C_{12} (GPa)	122.7	125	148.5 ± 10	154	130	121	127	139.4
C_{13} (GPa)	91.8	120	98.9 ± 3.5	84	122	93	97	121.5

to external deformation and occurs in many formulas describing diverse mechanical and physical characteristics. The shear modulus (G), however, recounts the resistance to shape change caused by a shearing force. In addition to B and G, the Young modulus (E) is the resistance to uniaxial tensions. These three distinct moduli (B, G, and E) are other useful parameters for defining the mechanical properties of materials [1, 2, 16, 17]. Fig. 2 displays the pressure behavior of B, G, and E of w-AlN for the entire range.

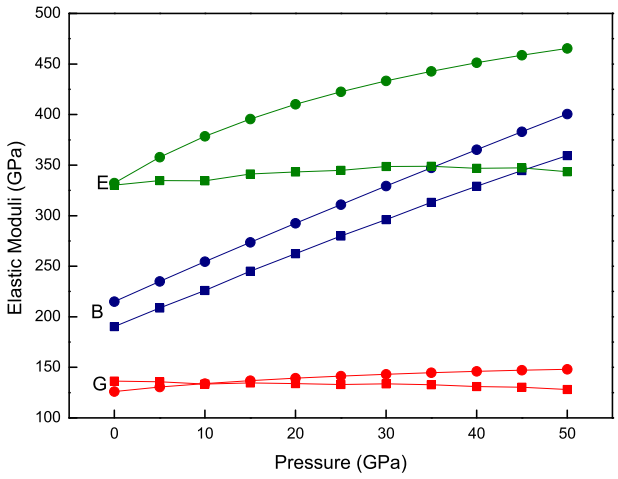

FIG. 2: Young's, bulk, and shear moduli of w-AlN.

As in Fig. 1, the circles represent our results, where squares are for the DFT data of the B, E, and G moduli. From the prevalent physical definition of the bulk modulus ($B = \Delta P/\Delta V$), it is expected to be increasing, because of its direct proportion to the applied pressure. Indeed, the bulk modulus of w-AlN exemplifies a straight increment as expected, and agrees to the DFT [6] data. Unlike the sharp increment in B, the E and G moduli have slight differences, and disagree with the previous DFT results under pressure.

Aside from the pressure behavior of these three moduli, Table II summarizes another numerical comparison for B, G, and E, the elastic moduli of the present and former data of w-AlN at 0 K and 0 GPa. The present results for the B, G, and E moduli agree both with the experiments and the DFT results, as seen in Table II.

TABLE II: Comparing the bulk, shear, and Young moduli of w-AlN with the previous and present results.

	Exp (Ref. [33])	Ref. [6]	Present
B (GPa)	210	190.38	214.94
G (GPa)	131	136.31	126.06
E (GPa)	308	330.14	332.14

The Poisson ratio (ν) is the ratio between the transverse strain (e_t) and longitudinal strain (e_l) in the elastic loading direction, and is used for evaluating the bonding behavior of materials [17]. For instance, the Poisson ratio (ν) for covalent materials is on the order of 0.1, whereas a typical value for ionic materials is 0.25 [32].

The Poisson ratio of w-AlN begins with 0.23 at zero pressure and shows a linear increment with increasing pressure denoted again with circles, as seen in Fig. 3.

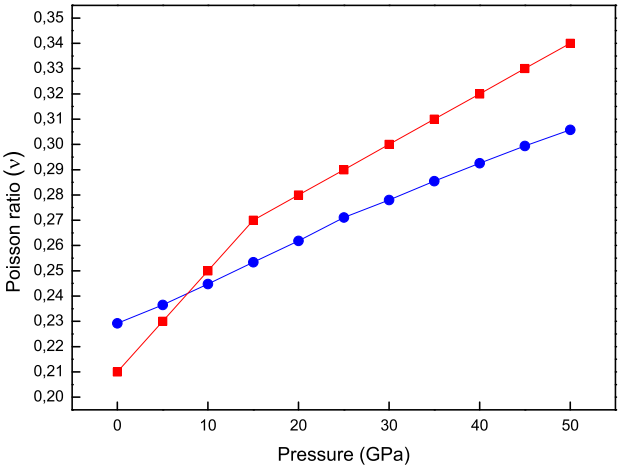

FIG. 3: Poisson ratio of w-AlN under pressure.

Despite the slight disagreement with DFT data (squares) under 10 GPa, our results have a similar curve behavior for ν above 15 GPa. Beyond this correspondence, typical relations between B and G are expressed as $G = 1.1B$ for covalent and $G = 0.6B$ for ionic materials [32]. After a careful assessment, we ascertained the relation of B and G to be

0.58 at $T = 0$ K and $P = 0$ GPa for w-AlN. Such two crosschecked results ($\nu = 0.23$ and $G = 0.58B$) manifest the ionic bonding characteristic of w-AlN analogous to former experiments [7] and DFT findings [33].

In solids, low temperature ($T = 0$ K in our case) acoustic modes can cause vibrational excitations. Depending on this fact, two typical elastic waves: longitudinal and shear waves exist. The velocity V_P symbolizes longitudinal wave velocity and V_S stands for the shear wave velocity [16, 17]. Fig. 4 shows the behavior of the V_P and V_S velocities for w-AlN as a function of pressure.

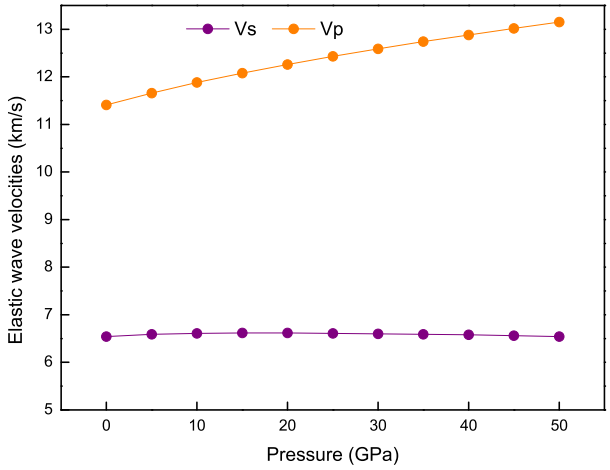

FIG. 4: Elastic wave velocities of w-AlN vs. pressure.

V_P has a more substantial increment than V_S, which is the observed circumstance for most materials. Obtained data, for both V_P and V_S, are again satisfactory when compared to previous experimental and DFT results [6].

Kleinman introduced a parameter (ζ) for materials, stating the relative ease of bond bending to bond stretching [26, 34]. According to Kleinman, minimizing bond bending leads to $\zeta = 0$, and minimizing bond stretching leads to $\zeta = 1$. After Kleinman, Harrison [35] proposed and approximated the Kleinman parameter for typical elastic constants with the expression $\zeta = C_{11} + 8C_{12}/7C_{11} + 2C_{12}$.

Fig. 5 shows the dependency of the Kleinman parameter upon the studied pressure range. The present results exhibit an intermediate value of the Kleinman parameter with 0.50 between bending and stretching for the ground state of w-AlN. Also ζ displays a linear increment with increasing pressure, which for this case leads to bond stretching in w-AlN.

The elastic anisotropy of crystals is crucial in engineering, since it correlates with the possibility to produce microcracks in materials. The anisotropy factor $A = 2C_{44}/(C_{11}-C_{22})$ can serve for a deeper outlook on the elastic anisotropy of w-AlN. For a completely isotropic material, A is equal to 1, while any value smaller or larger than 1 indicates anisotropy. The

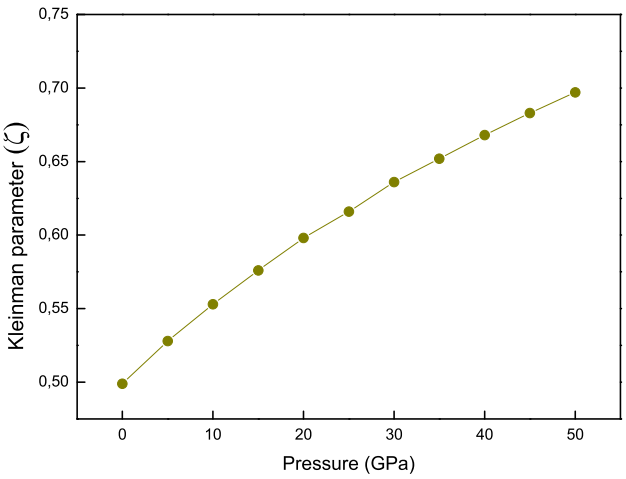

FIG. 5: Kleinman parameter of w-AlN against pressure.

magnitude of the deviation from 1 is a measure of the degree of elastic anisotropy possessed by the crystal [1, 37].

As seen in Fig. 6, the obtained anisotropy factors of w-AlN is close to or equal to 1 below 10 GPa, showing that w-AlN is isotropic between 0 GPa and 10 GPa. This behavior of w-AlN agrees with the low anisotropy concluded in DFT [6] calculations. It is also clear from Fig. 6 that the elastic anisotropy of w-AlN becomes more dominant above 10 GPa.

The dielectric constants of materials are fundamental optoelectronic parameters for device design for almost all fields of modern electronics and are responsible for the characteristics of the charge carriers, dopants, defects, impurities, insulators, and semiconductors [38].

The plots in Fig. 7 demonstrate the typical static (ϵ_0^{11} and ϵ_0^{33}) and high frequency (ϵ_∞^{11} and ϵ_∞^{33}) dielectric constants of w-AlN under pressure. Both static dielectric constants decrease with an increment of the applied pressure. On the other hand, a pressure increment does not much affect ϵ_∞^{11} and ϵ_∞^{33}, where both of them keep their continuous behavior under pressure, as seen in Fig. 7.

The obtained values of all dielectric constants are reasonable since the results are of about the measurements [26].

Overall, the obtained results display a fair agreement with the experiments, in particular for the elastic constants, elastic wave velocities, Poisson ratio, and dielectric constants. As well, the presented results for all considered parameters of w-AlN are not only consistent with the experiments, but are also better than those of some of the theoretical data.

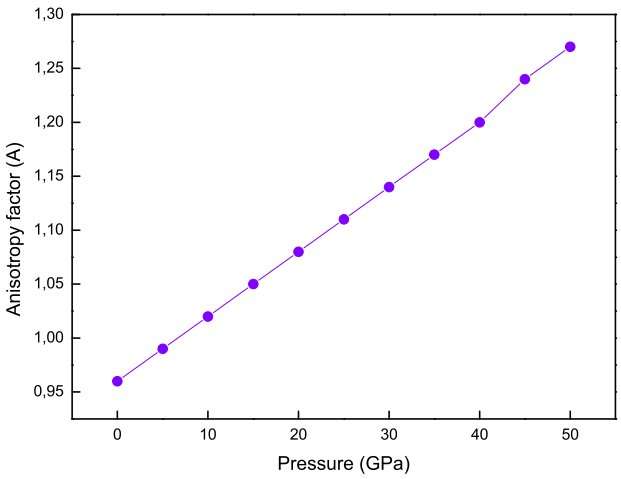

FIG. 6: Pressure dependency of the anisotropy factor for w-AlN.

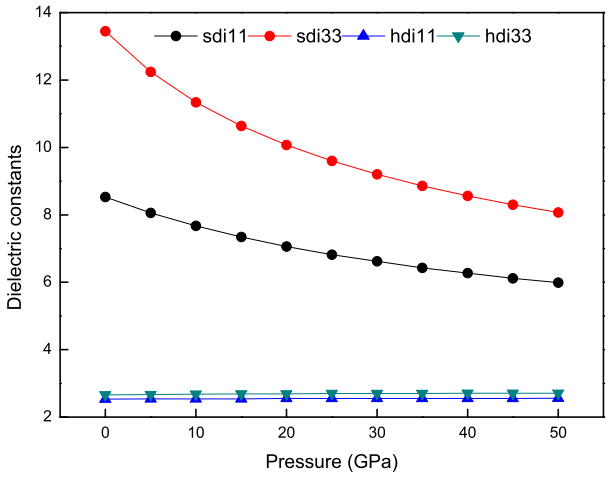

FIG. 7: Dielectric constants of w-AlN under pressure.

IV. CONCLUSION

In summary, we applied an existing shell model potential for the first time in conjunction with geometry optimization calculations to predict the high-pressure elastic properties of w-AlN. As our results demonstrate, application of a shell model potential that is origi-

nally used for predicting the ground state bulk, lattice, and defect properties of w-AlN [26] well reproduces other mechanical, optical, and elastic features of this material under pressure. In particular, the obtained results are consistent with the former experimental values for the elastic constants, Poisson ratio, elastic wave velocities, dielectric optical constants, and are better than those of some other published data. In addition to these findings, w-AlN shows an ionic bonding character for the entire surveyed pressure range, and elastic anisotropy begins above the pressures 10 GPa, similar to the DFT findings. We hope that the present results especially will be shedding further light on the future works regarding the high-pressure elastic and relevant characteristics of w-AlN.

References

[1] A. Maachou *et al.*, Comput. Mater. Sci. **50**, 3123 (2011). doi: 10.1016/j.commatsci.2011.05.038
[2] A. Djied *et al.*, Comput. Mater. Sci. **84**, 396 (2014). doi: 10.1016/j.commatsci.2013.11.041
[3] Z. Zhijiao *et al.*, Physica B **406**, 737 (2011). doi: 10.1016/j.physb.2010.11.040
[4] M. Magnuson *et al.*, Phys. Rev. B **80**, 155105 (2009). doi: 10.1103/PhysRevB.80.155105
[5] B. Dauodi *et al.*, Int. J. Nanoelectron. Mater. **1**, 65 (2008).
[6] W. Y. Liang *et al.*, Commun. Theor. Phys. **49**, 489 (2008).
[7] M. Pravica *et al.*, Phys. Stat. Sol. (b) **250**, 726 (2013). doi: 10.1002/pssb.201200485
[8] K. Tsubouchi and N. Mikoshiba, IEEE. Trans. Sonics Ultrason. Su. **32**, 634 (1985). doi: 10.1109/T-SU.1985.31647
[9] L. E. McNeil, M. Grimsditch, and R. H. French, J. Am. Ceram. Soc. **76**, 1132 (1993). doi: 10.1111/j.1151-2916.1993.tb03730.x
[10] A. F. Wright, J. Appl. Phys. **82**, 2833 (1997). doi: 10.1063/1.366114
[11] M. van Schilfgaarde, A. Sher, and A.-B. Chen, J. Cryst. Growth **178**, 8 (1997). doi: 10.1016/S0022-0248(97)00073-0
[12] S. Saib and N. Bouarissa, J. Phys. Chem. Solids **67**, 1888 (2006). doi: 10.1016/j.jpcs.2006.05.007
[13] F. Peng *et al.*, Physica B **403**, 4259 (2008). doi: 10.1016/j.physb.2008.09.013
[14] A. J. Wang *et al.*, Comput. Mater. Sci. **48**, 705 (2010).
[15] J. D. Gale, *Molecular modeling theory: applications*, (in the Geosciences) Eds. C. R. Timothy and J. D. Kubicki, 37 (Mineralogical Society of America, Washinton, D.C., 2001).
[16] E. Güler and M. Güler, Adv. Mater. Sci. Eng. **2013**, 525673 (2013).
[17] M. Güler and E. Güler, Chinese Phys. Lett. **30**, 056201 (2013). doi: 10.1088/0256-307X/30/5/056201
[18] J. D. Gale, J. Chem. Soc. Faraday **93**, 629 (1997). doi: 10.1039/a606455h
[19] J. D. Gale and A. L. Rohl, Mol. Simulat. **29**, 291 (2003). doi: 10.1080/0892702031000104887
[20] X. Q. Hu *et al.*, Physica B **405**, 2577 (2010). doi: 10.1016/j.physb.2010.03.035
[21] M. E. G. Valerio, R. A. Jackson, and J. F. de Lima, J. Phys. Condens. Mat. **12**, 7727 (2000). doi: 10.1088/0953-8984/12/35/308
[22] A. Walsh *et al.*, Chem. Mater. **21**, 4962 (2009). doi: 10.1021/cm902280z
[23] T. D. Archer *et al.*, Phys. Chem. Minerals **30**, 416 (2003). doi: 10.1007/s00269-002-0269-z
[24] A. P. Ayala, J. Phys. Condens. Mat. **13**, 11741 (2001). doi: 10.1088/0953-8984/13/50/334
[25] B. G. Dick and A. W. Overhauser, Phys. Rev. **112**, 90 (1958). doi: 10.1103/PhysRev.112.90
[26] J. A. Chisholm, D. W. Lewis, and P. D. Bristowe, J. Phys. Condens. Mat. **11**, L235–L239 (1999). doi: 10.1088/0953-8984/11/22/102

[27] G. C. Broyden, J. Inst. Math. Appl. **6**, 76 (1970). doi: 10.1093/imamat/6.1.76
[28] R. Fletcher, Comput. J. **13**, 317 (1970). doi: 10.1093/comjnl/13.3.317
[29] D. Goldfarb, Math. Comput. **24**, 23 (1970). doi: 10.2307/2004873
[30] D. F. Shanno, Math. Comput. **24**, 647 (1970). doi: 10.2307/2004840
[31] P. C. Ying *et al.*, Chinese Phys. B **23**, 026201 (2014). doi: 10.1088/1674-1056/23/2/026201
[32] A. Bouhemadou *et al.*, Comput. Mater. Sci. **45**, 474 (2009). doi: 10.1016/j.commatsci.2008.11.013
[33] F. Litimein *et al.*, New J. Phys. **4**, 64 (2002). doi: 10.1088/1367-2630/4/1/364
[34] http://www.ioffe.rssi.ru/SVA/NSM/Semicond/AlN/ and references therein.
[35] L. Kleinman, Phys. Rev. **128**, 2614 (1962). doi: 10.1103/PhysRev.128.2614
[36] W. A. Harrison, *Electronic Structure and the Properties of Solids*, (Dover Publications Inc, New York, 1980), Chap. 8.
[37] E. Güler and M. Güler, Mat. Res. [online]. ahead of print, pp. 0. Epub Aug 15, (2014). doi: 10.1590/1516-1439.272414
[38] D. Xue, K. Betzler, and J. H. Hesse, Phys. Condens. Mat. **12**, 3113 (2000). doi: 10.1088/0953-8984/12/13/319